FACTA UNIVERSITATIS (NIŠ)
SER.: ELEC. ENERG. vol. 24, no. 2, August 2011, 243-256

Analytical Estimation of Flux Waveforms In 8/6 Switched Reluctance Motors Based on Extension of Flux Tube Method

Dedicated to Professor Slavoljub Aleksić on the occasion of his 60th birthday

Mojtaba Babaei, Jawad Faiz, Maryam Bahramgiri, and Sohrab Amini

Abstract: This paper presents a novel analytical methodology to model the four-phase 8/6 switched reluctance motor (SRM) for determination of the magnetic flux waveforms within the different sections of the motor. For this, 2-D finite-element analysis (FEA) of the motor is carried out to identify the flux tube plot within the motor at different rotor positions. Equations for calculation of inductance and flux-linkage characteristics of the SRM stator winding are derived as function of the motor specifications, rotor position and the stator current excitation. Voltage equation is then used to obtain the variation of the excitation current versus rotor positions. This obtained current waveform is then used to extend the flux tubes method equations to dynamics mode. Consequently, a model of the 8/6 SRM can be formed via the non-linear dynamic equations to calculate the flux waveform within the stator poles. The results obtained using the analytical method is verified by FEA and actual measurement of the motor. It is shown that this method is capable to predict accurately the flux shape in different portions of the 8/6 SRMs for a given excitation current shape.

Keywords: Flux waveforms; FE analysis; flux tube method; 8/6 SRM.

1 Introduction

FLUX waveforms in various sections of SRMs should be known in order to calculate the losses within the motor core lamination. These flux waveforms are

Manuscript received on June 3, 2011.

M. Babaei is with Islamic Azad University, Shahre-Rey Branch, Tehran, Iran (e-mail: mba_babaei@yahoo.com). J. Faiz is with Center of Excellence on Applied Electromagnetic Systems, School of Electrical and Computer Engineering, University of Tehran, Tehran, Iran (e-mail: jfaiz@ut.ac.ir). M. Bahramgiri and S. Amini are with Niroo Research Institute, Tehran, Iran.

function of both rotor position and excitation current [1]. Calculations of the waveforms are complicated due to the deep saturation and non-sinusoidal excitation of the SRMs. At this end, different techniques have been so far introduced to find the patterns and determine the flux waveforms within the SRMs.

The first model to determine the stator poles flux waveforms was developed based on assumption that the waveforms have triangular shape [2]. The flux waveforms in other parts of the machine are then graphically determined. In [3], the flux waveform in one section of the stator yoke has been measured and it is then used to predict the flux waveforms in other parts of the SRM magnetic circuit. The core losses have been estimated by harmonic analysis of these waveforms. The error of the estimated core losses is due to ignoring the saturation effects in corner locations of the stator poles that happens because of a large number of passing flux lines. Alternative technique presents the ratio between the flux values in different sections of the magnetic circuit of the SRM in matrices form [4]. Accuracy of this method is reasonable, but their mathematical manipulation is too difficult. Approximation of flux waveforms with conventional equations by neglecting the saturation of the magnetic circuit of a three-phase 6/4 SRM has been presented in [5].

A 2D FEA has been used to evaluate the flux density waveforms in different parts of the motor [6]. These waveforms have been fitted to fourth-order polynomials to calculate core losses. This method necessitates an appropriate package to implement and generally it takes a long computation time. It also requires a large computer memory which is considered as disadvantages. Also, a linear approximation has been used to evaluate the flux waveforms in the motor by [7]. Previous papers have concentrated on the determination of the flux waveforms in SRMs which have disadvantages especially in complicatedly and/or precisely. This paper presents a new simple analytical method to resolve the drawbacks. FEA of a typical 8/6 SRM is applied in section II, and magnetic flux tubes in the motor is obtained and three regions based on the positions of the rotor in respect to the stator poles are defined. In section III, governing equations of magnetic flux tubes in the regions are derived to calculate inductance and flux-linkage characteristics of the motor. The voltage equation of the stator winding is then given in section IV. In this section, the inductance of the stator winding obtained in previous section is used to calculate the excitation current in different rotor positions. In section V, the nonlinear algebraic equations of the motor are extended to dynamics mode in which the excitation waveform is incorporated in the equations. These equations form the model of the 8/6 SRM to calculate the flux in stator pole versus rotor positions. This waveform is then used to predict the flux waveforms in various sections of the 8/6 SRM in section VI. Both FE and experimental results of actual 8/6 SRM are compared to the analytical results to verify the accuracy of the proposed method.

2 Magnetic Flux Tubes Within 8/6 SRM

In order to apply the flux tubes method, it is necessary to determine the flux lines within the SRM for different positions of rotor by the FEA of the motor. Here, a 8/6 SRM shown in Fig. 1 is analyzed. The motor specifications have been summarized in Table 1. In the FEA of the SRM, three regions are defined based on the angular position of rotor poles, θ. The three regions are, I) unaligned position up to the beginning of stator and rotor poles overlap (region I), II) beginning of overlapping up to the full overlapping (region II), and III) full overlapping position up to the aligned position (region III) [8]. Each region must be modeled by predominant number of flux tubes. Flux2D 10.2 software package is used for FEA [9], at constant excitation. The result obtained from the analysis has been shown in Fig. 2. It is observed that 10, 8 and 8 flux tubes is adequate to model regions I, II and III, respectively.

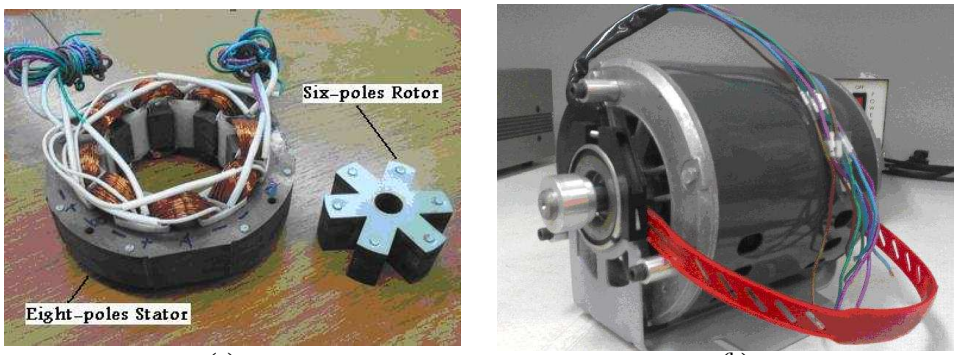

(a) (b)

Fig. 1. (a) Stator and rotor of 8/6 SRM, and (b) assembled 8/6 SRM.

Table 1. Specifications of the 8/6 SRM.

Quantity	Values	Quantity	Values
Stator outer diameter	157 mm	Rotor poles height	30.2 mm
Core diameter	78.7 mm	Air-gap length	0.35 mm
Shaft diameter	17 mm	Turns of winding	419/ph
Stack length	30 mm	DC link voltage	300 V
Stator poles arc	24°	Rated speed, N_r	1425 rpm
Rotor poles arc	27°	Stator and rotor lamination material	
Stator poles height	22.8 mm	:V800–50V	

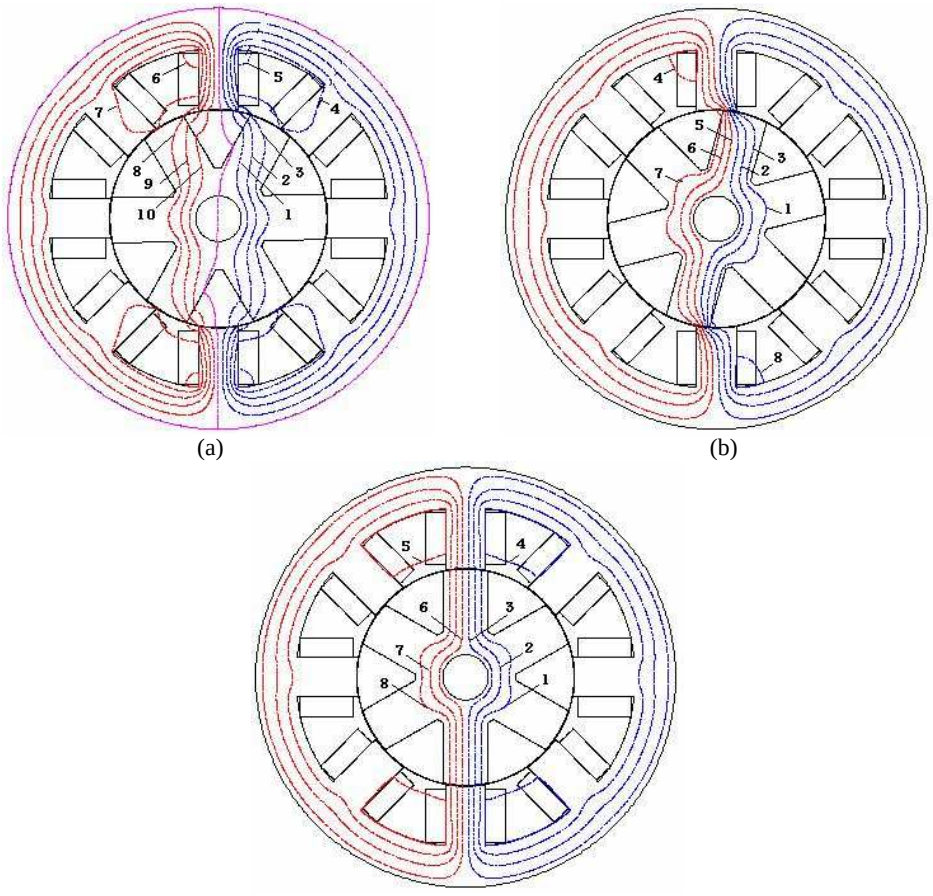

Fig. 2. Identification of flux tubes plot in three-regions using FEA of the 8/6 SRM from unaligned to aligned position: (a) region I, (b) region II and (c) region III.

3 Calculation of Flux-Linkage and Inductance Characteristics of 8/6 SRM

The magnetic circuit of the SRM is divided into five sections including stator poles, stator yoke, rotor poles, rotor core, and air gap. When the flux tubes are identified in three regions, it is possible to calculate the length and area of the flux tubes in each section. These lengths and areas of the flux tubes depend on the geometrical dimensions and rotor positions of the SRM.

The Ampere's law equation can be applied to each flux tube in various sections of the SRM. To demonstrate this, consider the flux tube1 in region III. Fig. 2c shows that the flux tube1 passes through the stator pole (sp), air-gap (g), rotor pole

(rp), rotor core (rc), and stator yoke (sy). Therefore, the Ampere's equation of the path is as follows:

$$\begin{aligned} N_{ph}i =& 2H_{sp}(\theta,i)l_{sp}(\theta) + 2H_{rp}(\theta,i)l_{rp}(\theta) \\ &+ \frac{B_g(\theta,i)A_g(\theta)}{P_g(\theta)} + H_{sy}(\theta,i)l_{sy}(\theta) + H_{rc}(\theta,i)l_{rc}(\theta) \end{aligned} \tag{1}$$

where N_{ph}, H and l are the number of winding turns, magnetic field intensity and length of the flux tubes in each section of the motor, respectively. P_g and A_g are the permeance and area of the flux tube in the air-gap and i recall the excitation current. Therefore, 10, 8 and 8 nonlinear algebraic equations can be derived to model the region I, II, and III, respectively. These equations are the function of the motor specifications, rotor position and stator winding excitation.

To solve the above nonlinear equations and obtain the stator pole flux, assumed an initial value of the stator pole flux and evaluate the flux density (B) in various sections of the motor corresponding to the paths of the flux tube. Then, from the magnetization characteristic of the lamination, the corresponding magnetic field intensity (H) of each section, can be determined. Consequently, the magnetomotive force (MMF) of each section is calculated and Ampere's law equation associated with each flux tubes is well established. The MMF due to the excitation current must be equal to the previous calculated permissible MMF or the error between them is within the predefined limit. Therefore, the iterative process with the modified stator pole flux continues up to converging to the solution. Following the calculation of the stator pole flux, the corresponding inductance for each flux tube is evaluated. The inductance of flux tubes 10, 8, and 8, in three regions are summed up to get the phase inductance in three regions, respectively. Once the phase inductance characteristic, $L(\theta,i)$, is obtained, the flux-linkage characteristic can be estimated.

The above analytical method is implemented by the MATLAB script to calculate the phase inductance and flux-linkage in different regions of the 8/6 SRM. In this case, the displacement of the rotor between the unaligned (0°) and the aligned (30°) position is considered and excitation current level is statically changed to 1.3 times of the motor rated current.

Fig. 3 shows the flux-linkage of the 8/6 SRM obtained by the proposed analytic method and actual measurement. The effect of the magnetic saturation in the rotation of the rotor from the unaligned position to the aligned position is fully clear. It is also observed that the results of application of the proposed method are in good agreement with the measured value, especially at low excitation up to the rated current; where there is no deep saturation.

Table 2 compares the phase inductance in unaligned, 10°, 20°, and aligned positions at rated excitation current that calculated using the analytical and FE methods,

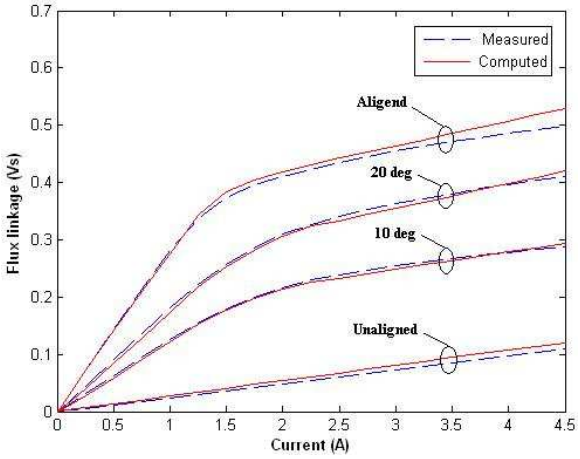

Fig. 3. Flux linkage characteristic of the 8/6 SRM obtained using proposed analytic method and measurement.

while the measured value is also present. Table 2 indicates that the results obtained using the analytical method is in good agreement with those obtained from FEA and measurement. It is also clear that the error at the unaligned position is larger than that of the 10°, 20°, and aligned positions. The reason is the leakage flux passing through all the adjacent areas and less accuracy to estimate the flux tubes geometry due to the complicated shapes. Therefore, modeling this region requires considering more flux tubes for computation of the actual inductance. While the absolute values of the phase inductance at the unaligned position are too low, the effect of this error in the stator pole flux waveform estimation is negligible.

Table 2. Inductance at various rotor positions with 3.797 A excitation.

Rotor Position	Analytical [MH]	FE [MH]	Measured [MH]
Unaligned (0°)	29.8	28.2	27
10°	75.5	76.2	76.8
20°	10.5	105.7	106.1
Aligned (30°)	143.3	140.2	138.5

4 Excitation Current Versus Rotor Angular Position

To determine the flux in the stator poles of the SRM versus rotor position, it is necessary to estimate the excitation current in every rotor position. For this, assume that the SRM is rotating with the rated speed, N_r, and the dc link voltage, V_{dclink},

has been applied to the stator winding at rotor position angle θ_r. In such a case, rotor travels any degree at time $t_s = 1/6N_r$ and inductance variation in this time can be constant. The current equation at position $\theta_r + 1$ is then calculated from the voltage equation as follows:

$$i(\theta_r + 1) = \frac{V_{dclink}}{R_{st}} \left(1 - e^{-\frac{R_{st}}{L_{\theta_r}} t_s}\right) \tag{2}$$

where R_{st} is the resistance of the stator phase winding. Also, L_{θ_r} is the minimum inductance of the stator winding at rotor position of θ_r that can be obtained from $L(\theta, i)$ characteristic. The current equation at rotor position $\theta_r + 2$ is then calculated as follows:

$$i(\theta_r + 2) = -\frac{V_{dclink}}{R_{st}} \left(1 - e^{-\frac{R_{st}}{L_{\theta_r+1}} t_s}\right) + i(\theta_r + 1) e^{-\frac{R_s}{L_{\theta_r+1}} t_s} \tag{3}$$

where $L(\theta_r + 1)$ is the inductance of the stator winding at rotor position $\theta_r + 1$ and current $i(\theta_r + 1)$ that can be precisely extracted also from $L(\theta, i)$ characteristic. This trend continues for rotor position $\theta_r + 2$ and further up to the rated current. At this rotor condition, current remains constant up to the phase commutation angle, θ_c, and at this angle, the reversed dc bus voltage is applied to the phase winding. Therefore, the winding current begins to drop and the current equation at position $\theta_c + 1$ can be expressed as follows:

$$i(\theta_c + 1) = -\frac{V_{dclink}}{R_{st}} \left(1 - e^{-\frac{R_{st}}{L_{\theta_c}} t_s}\right) + i_{peak} e^{-\frac{R_{st}}{L_{\theta_c}} t_s} \tag{4}$$

This trend continues up to zero current and completing the commutation process. Fig. 4 shows the obtained current waveforms of the four-phase of the 8/6 SRM.

Fig. 5 shows the control block diagram of one phase of the 8/6 SRM designed for experimental setup. The control strategy starts from Φ_A signal that generated by the position sensor in order to determine the condition of low switch. While the blade slot is located in the front of the phase sensor, the sensor generates a low signal level that passes through the NOT gate and on-state command produces for low switch. In this condition, the PWM signal that cause to generate and control of the phase current, is applied to the high switch of the phase. Also, the phase current is set to the reference current with the duty cycle control of the PWM signal. The reference current is calculated based on the error between the actual speed and reference speed. The average value of the PWM signal is obtained with an integrator (low-pass filter) and reference current is generated.

The sensors board on the SRM shaft and the actual drive for implementing the control strategy and actual measurement has been shown in Fig. 6. It is clear that

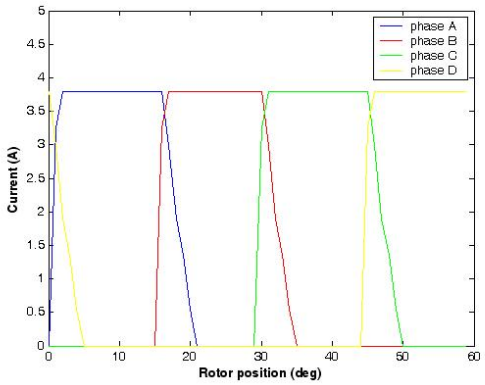

Fig. 4. Four-phase excitation current of the 8/6 SRM obtained using proposed analytic method.

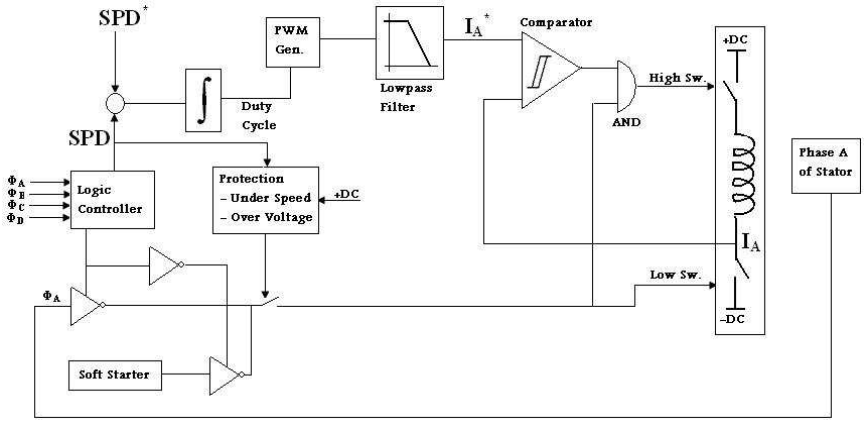

Fig. 5. Control block diagram of one phase of 8/6 SRM.

two IGBT switches are considered for each phase of the motor. The 8/6 SRM has been driven at the rated rotation speed of 1425 rpm and the control strategy is set to regulate the peak current value to 3.797A, the duration time (or positions) of the fixed excitation current and the commutation angle. Fig. 7 shows the measured instantaneous excitation current waveform of the two-phase of the SRM. As shown in Fig. 4 and Fig. 7 when the control strategy setting is to be implemented using some assumptions in calculating the current waveform, a good agreement between the result of the measurement and predicted current in every rotor positions is achieved.

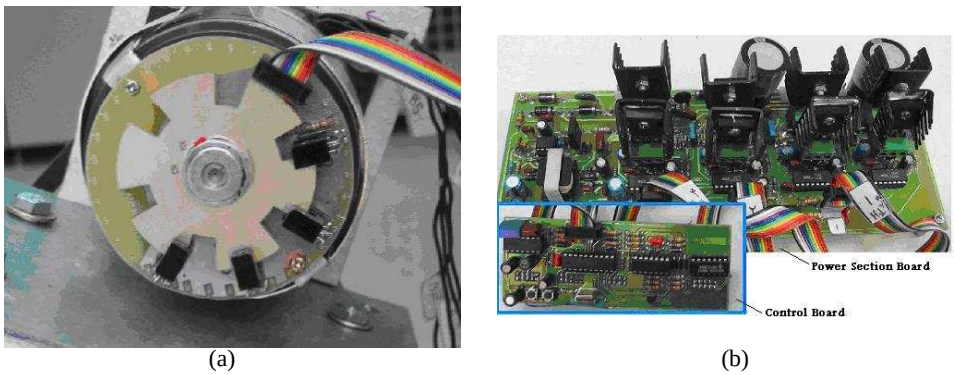

(a) (b)

Fig. 6. ((a) Sensors board mounted on the 8/6 SRM shaft, and (b) 8/6 SRM drive for measurement purpose.

5 Flux Waveform of Stator Pole

When the excitation current at each rotor position between unaligned to aligned position is obtained, it is possible to extend the Ampere's low equations to dynamics mode of operation of SRM. It means that the constant excitation current should be substituted by this current waveform in the above mentioned nonlinear equations. Therefore, the Ampere's equation of the flux tube 1 in region III described by (1) in static form, is extended to (5) in which the $i(\theta)$ incorporates into the equation for the above mentioned goal, as follows:

$$\begin{aligned} N_{ph}i(\theta) =& 2H_{sp}(\theta, i(\theta))l_{sp}(\theta) + 2H_{rp}(\theta, i(\theta))l_{rp}(\theta) + \frac{B_g\theta, i(\theta)A_g(\theta)}{P_g(\theta)} \\ &+ H_{sy}(\theta, i(\theta))l_{sy}(\theta) + H_{rc}(\theta, i(\theta))l_{rc}(\theta) \end{aligned} \tag{5}$$

This has been implemented for the all flux tubes in the regions and a set of nonlinear equations describes all effects of the rotor poles rotation from the unaligned to aligned positions (in respect to the stator pole) in three regions. These effects include the shape and paths of the each flux tubes, rotor positions and the real excitation current at any rotor position. The waveform of $i(\theta)$ (Fig. 4), has been used to drive the model. This model solves using an iteration method with very low convergence rate and fluxes in stator pole (between unaligned and aligned positions) are calculated. Fig. 8 compares the flux waveform of the stator pole with the measured waveform. It is observed the flux is zero in the stator pole for rotor position of 21° to aligned position due to the zero excitation current in this region.

For better comparison, Table 3 gives the flux in the stator pole of the 8/6 SRM as a function of both rotor position and the excitation current that obtained using the proposed analytic method, FEA and measurement. It is found that the results

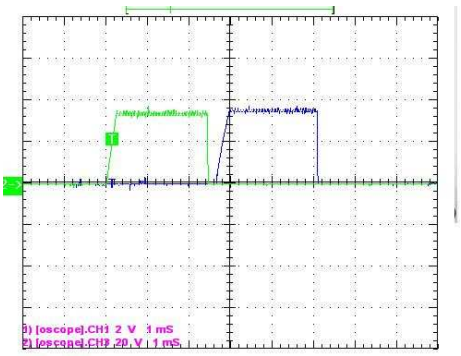

Fig. 7. Measured instantaneous excitation current waveform of two-phase of 8/6 SRM.

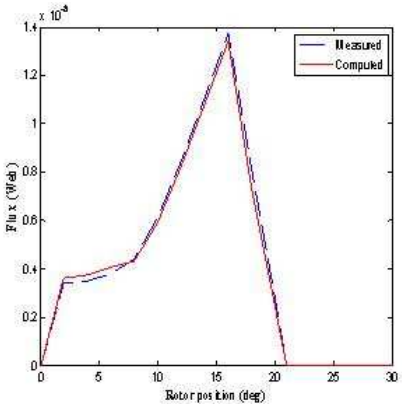

Fig. 8. Comparison of flux waveform in stator pole of 8/6 SRM obtained using new analytical method and measurement.

obtained using the new method is fairly in agreement with those obtained by the FEA and measurement. When the flux waveform at the stator pole of the SRM is obtained, the flux waveforms in various magnetic sections of the SRM can be calculated.

Table 3. Flux of stator pole of 8/6 SRM as a function of rotor positions $[\theta]$, and excitation current [A]

	Analytic		FE		Measured	
θ	A	mWb	A	mWb	A	mWb
0°	0	0	0	0	0	0
2°	3.797	0.3617	3.05	0.3510	3.797	0.3411
4°	3.797	0.3745	3.797	0.3569	3.797	0.3483
6°	0.797	0.4068	3.797	0.3991	3.797	0.3801
8°	3.797	0.4330	3.797	0.4373	3.797	0.4403
10°	0.797	0.5930	3.797	0.6020	3.797	0.6131
12°	0.797	0.8260	3.797	0.8401	3.797	0.8472
14°	0.797	1.081	3.797	1.089	3.797	1.105
16°	3.797	1.341	3.797	1.352	3.797	1.373
18°	1.898	0.7273	1.988	0.7815	1.841	0.8087
20°	0.542	0.2396	0.612	0.2612	0.521	0.2708
21°	0	0	0	0	0	0

6 Flux Waveforms within Various Sections of 8/6 SRM

Flux waveforms have different shape within the iron sections of the SRMs. Here, 16 distinct iron sections for 4-phase 8/6 SRM are considered to evaluate the flux waveforms. Fig. 9 shows different sixteen sections in the 8/6 SRM. The flux waveforms are derived starting from the stator poles of SRM. In 8/6 SRMs, each pole of the stator excited six times over a complete revolution of the rotor. Therefore, with

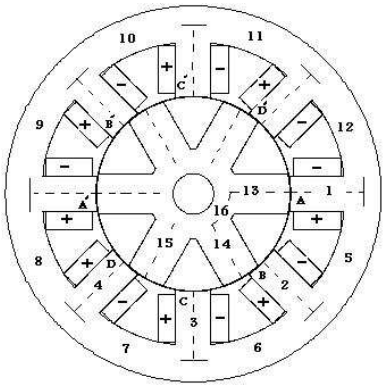

Fig. 9. Various sections of 8/6 SRM iron core for evaluation of flux waveforms.

the use of the flux waveform within one pole of the stator poles, (section 1), is shown in Fig. 8; it is possible to calculate the pole flux waveform in full revolution of the rotor. Other stator poles, sections 2, 3, and 4, would have the similar waveforms but would be offset by 15° in 8/6 SRM. Also, the diametrically opposite pole would have a similar waveform except that the polarity is reversed. They have the following identical frequency:

$$f_s p = \frac{N}{60} N_r = \frac{1425}{60} \times 6 = 142.5\ [Hz] \tag{6}$$

where N and N_r are the number of rotor poles and the rotor speed in revolution per minute (rpm), respectively.

The flux of the stator yoke varies from portion to portion based on the activated phase. Therefore, when the waveforms are calculate in the 8-poles of the stator, the waveforms are predictable in the 8-portions of the stator yoke. The flux waveform in section 5 of stator yoke can be obtained from sum of the flux waveforms of four stator poles. The sum of flux waveforms in stator poles 1, 2, and 3 minus 4, gives the waveform of section 6 of the stator yoke. Also, the sum of flux waveform in stator poles 1 and 2, minus the flux from sum of the waveforms in 3 and 4, gives the flux waveform in section 7 of the stator yoke. Finally, subtracting pole 1 from the sum of fluxes in poles 2, 3 and 4 will give the flux waveform in section 8 of stator

yoke. Due to the symmetry in stator yoke, the impact 0.5 should be considered in determining the stator yoke flux waveforms. Fig. 10 shows the flux waveforms of the stator yoke sections 5 to 8, over a full revolution of the rotor obtained using the proposed method. It is observed that the waveforms in sections 6, 7, and 8 have the same frequency with the flux frequency in the stator poles.

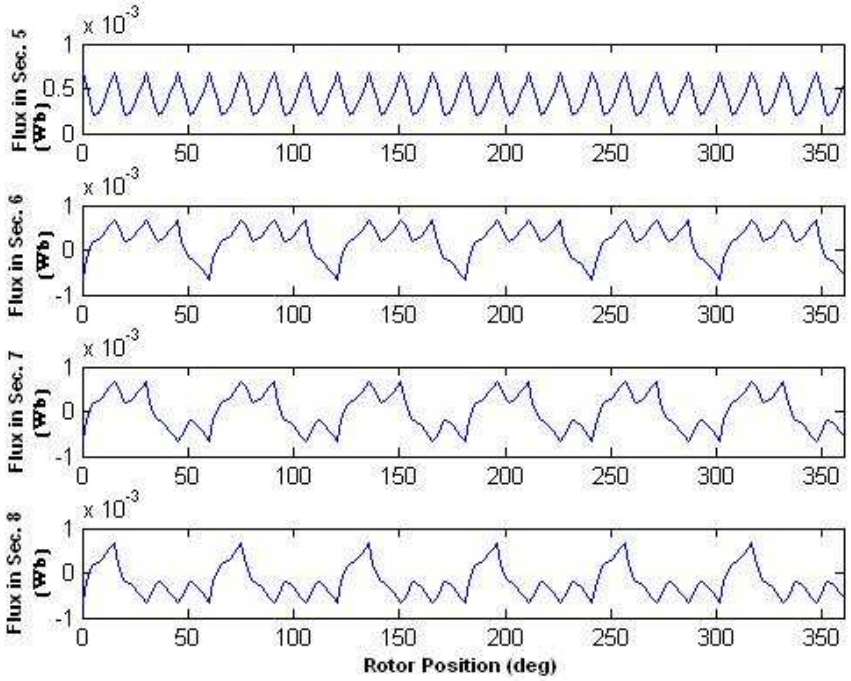

Fig. 10. Flux waveforms of stator yoke of 8/6 SRM over a complete revolution of rotor.

But, section 5 waveform has ripple with frequency of 4×142.5 Hz. The corresponding diametrically opposite sections of stator yoke; 9, 10, 11, and 12 have the reverse polarities with the waveforms of the sections 5, 6, 7, and 8, respectively.

The flux waveform in rotor pole has the frequency of 23.75 Hz and can be obtained from the stator pole flux. The flux waveform of one rotor pole, section 13, has been shown in Fig. 11 (top). Other rotor poles, sections 14 and 15, would have the similar waveforms but would be offset by 15° in 8/6 SRM. Also, the diametrically opposite pole would have a similar waveform except that the polarity would be reversed.

When the waveforms are calculated in the six rotor poles, the waveform is predictable in the rotor core. The flux waveform experienced by one of six portions of the rotor core over a full revolution has been represented in Fig. 11 (bottom). The other sections have the identical waveforms but are offset by 60° in 8/6 SRM.

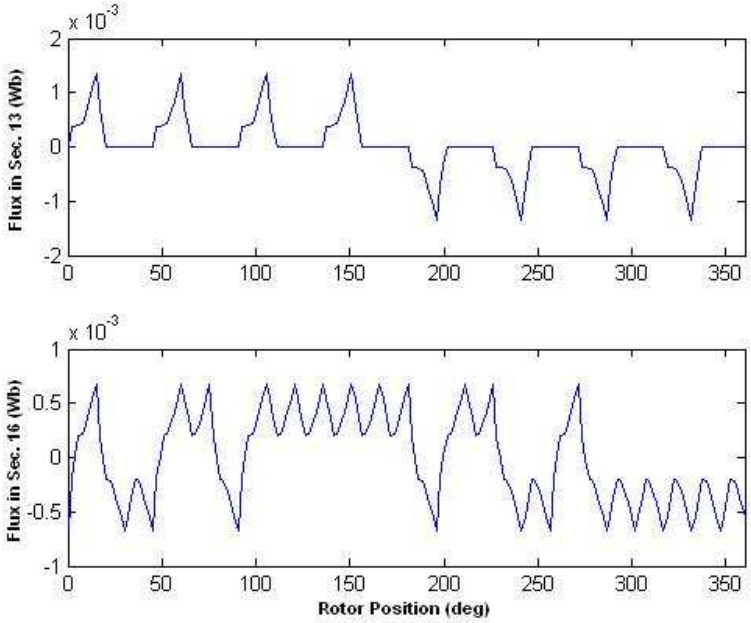

Fig. 11. Flux waveforms of rotor pole (top), and rotor core (bot-tom) of 8/6 SRM over a complete revolution of rotor.

The same frequency of 23.75 Hz is also observed in this waveform.

7 Conclusion

In this paper an analytic method was proposed to determine the flux waveforms in various sections of the 8/6 SRM. First, FEA of a typical 8/6 SRM was carried out using Flux2D 10.2 software package to identify the flux tubes at three regions. Amperes equation for all magnetic flux tubes in every region is then followed in non-linear forms that depend on the specifications of the motor, rotor position and excitation current. These nonlinear equations were solved using an iterative method to obtain the inductance and flux-linkage characteristics of the motor in different rotor positions and different excitation current. With the use of the inductance characteristic and extended volt-age equation, the phase excitation current at each rotor position is calculated. In this case the real excitation current waveform was incorporated into the nonlinear equations and the SRM model for calculation of the stator pole flux waveform was established. Other waveforms then calculated using the stator pole flux waveform. The results obtained by the proposed analytic method are as good as those obtained by the FE analysis and measured results.

Acknowledgement

The authors would like to thank Niroo Research Institute, Tehran, Iran for financial support of the project.

References

[1] J. Faiz and S. Pakdelian, "Finite-element analysis of a switched reluctance motor under static eccentricity fault," *IEEE Trans. on Magnetics*, vol. 42, no. 8, pp. 2004–2008, Aug. 2006.

[2] P. Materu and R. Krishnan, "Estimation of switched reluctance motor losses," in *Conf. Rec. IEEE-IAS Annu. Meeting*, Pittsburgh, PA, Oct. 13–18, 1988, pp. 79–90.

[3] J. Faiz and M. B. B. Sharifian, "Core losses estimation in multiple teeth stator pole switched reluctance motor," *IEEE Trans. on Magnetics*, vol. 30, no. 2, pp. 189–195, Mar. 1994.

[4] Y. Hayashi and T. J. E. Miller, "A new approach to calculation core losses in the srm," *IEEE Trans. on Ind. Application*, vol. 31, no. 5, pp. 1039–1046, Sept. / Oct. 1995.

[5] R. Krishnan, *Switched Reluctance Motor Drives: Modeling, Simulation, Analysis, Design and Applications*. CRC Press, 2001.

[6] P. Vijayraghavan, "Design of switched reluctance motors and development of a universal controller for switched reluctance and permanent brushless dc motor drives," Ph.D. dissertation, Virginia Tech, 2001.

[7] L. T. Mothomben and P. Pillay, "Lamination core losses in motors with non-sinusoidal excitation with particular reference to pwm and srm excitation waveforms," *IEEE Trans. on Energy Conversion*, vol. 20, no. 4, pp. 836–843, Dec. 2005.

[8] N. K. Sheth and K. R. Rajagopal, "Calculation of the flux-linkage characteristics of a switched reluctance motor by flux tubes method," *IEEE Trans. on Magnetics*, vol. 41, no. 10, pp. 4069–4071, Oct. 2005.

[9] *Flux2D 10.2 User Guide*, 2007.